Solar-Terrestrial Physics. 2023. Vol. 9. Iss. 2. P. 81–87. DOI: 10.12737/stp-92202310. © 2023
O.A. Danilova, N.G. Ptitsyna, M.I. Tyasto, V.E. Sdobnov. Published by INFRA-M Academic Publishing House

UDC 523-62, 523.9
DOI: 10.12737/stp-92202310

Received February 22, 2023
Accepted April 03, 2023

VARIATIONS IN COSMIC RAY CUTOFF RIGIDITIES DURING THE MARCH 8–11, 2012 MAGNETIC STORM (CAWSES II PERIOD)

O.A. Danilova
Institute of Terrestrial Magnetism, Ionosphere, and Radio Wave Propagation, St. Petersburg Branch, RAS, St. Petersburg, Russia, md1555@mail.ru

N.G. Ptitsyna
Institute of Terrestrial Magnetism, Ionosphere, and Radio Wave Propagation, St. Petersburg Branch, RAS, St. Petersburg, Russia, nataliaptitsyna@ya.ru

M.I. Tyasto
Institute of Terrestrial Magnetism, Ionosphere, and Radio Wave Propagation, St. Petersburg Branch, RAS, St. Petersburg, Russia, mtyasto@mail.ru

V.E. Sdobnov
Institute of Solar-Terrestrial Physics SB RAS Irkutsk, Russia, sdobnov@iszf.irk.ru

Abstract. The geomagnetic cutoff rigidity of cosmic rays (CRs) is the main factor regulating the arrival of CR particles at a given point on Earth's surface or inside the magnetosphere. To study the relationship between cutoffs and near-Earth space parameters, we have selected the strongest magnetic storm that occurred on March 8–11, 2012 during the CAWSES-II interval, recommended by SCOSTEP for detailed studies of solar-terrestrial relations. We have found the geomagnetic cutoffs by two methods: 1) by trajectory calculations in the magnetic field of the perturbed magnetosphere according to the Ts01 model and 2) by the spectrographic global survey method according to the data from the world network of neutron monitors. The largest drop in the cutoffs (−1.1 GV) obtained by the latter method was observed during the recovery phase of the storm. Apparently, this is due to the influence of the supersubstorms that occurred at that time. The analysis has shown that the closest connection of variations in the cutoffs can be traced with the geomagnetic activity index *Dst*, which indicates the determining contribution of the ring current to the transport of CRs. In addition, we have found a significant connection with the electromagnetic field parameters (with the B_z component of the interplanetary magnetic field and the azimuthal component of the electric field E_y). The dynamic solar wind parameters practically do not control variations in CR geomagnetic cutoff rigidities.

Keywords: geomagnetic threshold, cosmic rays, supersubstorm, interplanetary magnetic field, geomagnetic activity.

INTRODUCTION

Global climate changes in recent decades have stimulated the search for mechanisms of the influence of various space weather factors on Earth's weather and climate. One of the important factors on which space weather depends is cosmic rays (CRs). Variations in CR fluxes cause atmospheric ionization, which is associated, in particular, with such processes as formation of clouds, thunderstorms, and tropical hurricanes [Carslaw et al., 2002; Makrantoni et al., 2013]. The period of March 7–17, 2012 was recommended by SCOSTEP for in-depth studies into the space weather effects in the Sun–Earth system during disturbances. This period is called CAWSES-II (The Climate and Weather of the Sun–Earth System). During the active period of CAWSES-II, four geomagnetic storms were observed: on March 7, 9, 12, and 15 [Tsurutani et al., 2014]. These storms were generated by solar flares and related coronal mass ejections (CMEs) from the solar active region 1429AR and attendant interplanetary structures (shock fronts, compression regions ahead of interplanetary CMEs and magnetic clouds). These structures when reaching Earth followed each other and partially overlapped.

Geomagnetic cutoff rigidities R (geomagnetic thresholds) are the main factor regulating the CR arrival at a given point on Earth's surface or inside the magnetosphere. Variations in CR fluxes in the magnetosphere during magnetic storms are generally caused by variations in the geomagnetic cutoff rigidity ΔR and asymptotic directions of the arrival of particles at a given point in the magnetosphere [Dorman, 1963]. In turn, R depends on shielding properties of the geomagnetic field. Geomagnetic storms suppress geomagnetic shielding owing to a decrease in the strength of the field inside the magnetosphere due to the formation of ring current, magnetopause currents, magnetotail, and high-latitude field-aligned currents. As a result, cosmic particles can penetrate to lower latitudes.

Knowledge of the dependence of ΔR on solar wind (SW) and magnetospheric parameters can clarify some aspects of the SW—magnetosphere coupling and the accompanying geomagnetic effects that regulate the CR transport through the magnetosphere and atmosphere during magnetic storms. For the study, we have selected the strongest magnetic storm in the CAWSES-II period, the maximum of which was observed on March 9, 2012 ($Dst\sim$ – 143 nT).

The purpose of this paper is to study variations in geomagnetic thresholds during the March 8–11, 2012 storm, as well as their relationship with SW, interplanetary magnetic field (IMF), and geomagnetic activity parameters. This paper is a sequel to [Ptitsyna et al.,

This is an open access article under the CC BY-NC-ND license

2019, 2020, 2021], where variations in CR geomagnetic cutoff rigidities during severe storms have been studied. For each of these storms, correlations have their own unique character, so it is important to analyze as many strong storms as possible and create a database to identify common patterns. A new element of this work is that we analyze correlations of variations in geomagnetic thresholds with interplanetary parameters and geomagnetic activity indices during each of the three phases of storm development during the CAWSES-II period and delve into the latitude effect of these variations.

1. METHODS AND DATA

Variations in CR geomagnetic cutoff rigidities (geomagnetic thresholds) ΔR during this storm have been calculated by two methods.

The former is the spectrographic global survey (SGS) method, which determines rigidities R_{sgs} from observations made at the worldwide neutron monitor network [Dvornikov et al., 2013]. The SGS method is based on examining the processes of changing the energy of charged particles in regular electromagnetic fields of the heliosphere. The SGS method provides information on the distribution of primary CRs by energy and pitch angles in IMF, on changes in the planetary system of geomagnetic cutoff rigidities for each observation hour from ground observations of cosmic rays at the worldwide network of stations. This circumstance makes it possible, along with phases of the first and second harmonics of pitch-angle anisotropy, to identify the rigidity spectrum of isotropic component and the CR anisotropy, to obtain information about IMF orientation from the pitch-angle anisotropy phase, to determine variations in the planetary system of geomagnetic cutoff rigidities; observations of unstable charged CR components allow us to determine temperature characteristics of the atmosphere at the points of detection of these components per observation hour or at shorter time intervals. Table 1 lists (depending on statistical errors in measurements of neutron I_{nm} and charged I_{mt} CR components) standard errors in the values determined by the SGS method from ground observations of CRs: differential rigidity spectrum A_0, amplitudes A_1 and A_2 of CR pitch-angle anisotropy, ΔR_c variations, IMF longitudinal λ and latitudinal Ψ angles, mass average ΔT_{ma} and surface ΔT_{surf} atmospheric temperatures.

Variations in threshold geomagnetic cutoff rigidities were calculated using data from the worldwide network of CR stations with an hourly accumulation period [http://www01.nmdb.eu/data]. Hereinafter, the variations in ΔR_{sgs} obtained by this method will be referred to as observed.

The latter method of determining geomagnetic cutoff rigidities is based on the numerical calculation of particle trajectories in the model magnetic field of the magnetosphere [Shea et al., 1965]; in this case, the accuracy in determining the geomagnetic thresholds R_{ef} depends on the accuracy of the magnetospheric model. In this paper, we apply the semi-empirical model Ts01 of the magnetospheric magnetic field, designed for strong magnetic disturbances (see [Tsyganenko et al., 2003] and references therein). According to this model, the magnetic field inside the magnetosphere (without the main magnetic field) is the sum of contributions from the main magnetospheric current systems. Current systems in the Ts01 model were parameterized using satellite data acquired during 37 geomagnetic storms with $Dst \leq -65$ nT [Tsyganenko et al., 2003]. The model includes Chapman—Ferraro currents, which hold the geomagnetic field inside the boundary of the magnetosphere, symmetric and partial ring currents, transverse tail currents, and large-scale field-aligned currents. In order to bound the field inside the magnetosphere, the model includes a block describing the interaction field that reflects the effect of IMF penetration into the magnetosphere. The interaction field is represented as a homogeneous magnetic field proportional to the transverse component and directed along it. To calculate the magnetic field of internal sources, we use a representation of the main geomagnetic field in the form of series expansion in spherical harmonic functions up to $n=10$. Input parameters of the Ts01 model are the *Dst* variation, the SW density and velocity, as well as IMF components. The geomagnetic cutoff rigidity variations ΔR_{ef} obtained by this method will be called model.

We have made the calculations for each hour for the following stations: ESOI (33.30° N, 35.80° E), Almaty (43.20° N, 76.94° E), Rome (41.90° N, 12.52° E), Irkutsk (52.47° N, 104.03° E), Moscow (55.47° N, 37.32° E), and Kingston (42.99° S, 147.29° E). The stations were selected so that to cover under quiet conditions the main region of threshold rigidities R_c affected by the geomagnetic field: ESOI (10.8 GV), Almaty (6.61 GV), Rome (6.24 GV), Irkutsk (3.66 GV), Moscow (2.39 GV), and Kingston (1.88 GV). The geomagnetic thresh old variations were calculated in terms of the quiet-time average rigidities calculated on January 8, 2012.

Table 1

Standard errors of values found by the SGS method
for different statistical errors in neutron monitor and meson telescope data

I_{nm}, %	I_{mt}, %	λ, degree	Ψ, degree	A_0, %	A_1, %	A_2, %	ΔR_c, GV	T_{surf}, °C	T_{ma}, °C
±0.1	±0.1	±16.9	±21.5	±1.0	±8.8	±1.7	±0.03	±1.3	±0.3
	±0.2	±16.9	±21.5	±1.0	±8.8	±1.7	±0.03	±2.5	±1.2
±0.15	±0.1	±17.0	±21.8	±1.3	±8.8	±1.7	±0.04	±1.3	±0.3
	±0.2	±17.0	±21.8	±1.3	±8.8	±1.7	±0.04	±2.5	±1.0
±0.2	±0.1	±17.5	±22.1	±1.6	±8.9	±1.8	±0.05	±1.3	±0.3
	±0.2	±17.5	±22.1	±1.6	±8.9	±1.8	±0.05	±2.5	±1.0

Then we computed the correlation coefficients k of ΔR_{sgs} and ΔR_{ef} with SW, IMF, and geomagnetic activity parameters for the above stations. The parameters for which we determined the correlation with the geomagnetic thresholds are as follows: the B_z and B_y components, as well as total IMF B; the azimuthal component of electric field E_y, the SW velocity V, density N, pressure P, and the geomagnetic activity indices Dst and K_p. These parameters have been taken from the website [https://omniweb.gsfc.nasa.gov/form/dx1.html].

2. RESULTS

2.1. Behavior of cutoff rigidities and parameters of near-Earth space

Figure 1 shows model geomagnetic cutoff rigidity variations ΔR_{ef} (*a*) and observed ones ΔR_{sgs} (*b*) for March 8–11, 2012 for the stations under study, which are located at different latitudes, as well as electromagnetic field parameters (E_y, B_z, B_y), SW (V and P), and Dst variations (*c*–*h*).

The geomagnetic storm began after the arrival of an interplanetary magnetic cloud and the turn of IMF B_z to the south [Tsurutani et al., 2014]. The storm reached its maximum intensity (Dst=−143 nT) on March 9 at 08:00 UT (Figure 1), which can be attributed to Bz=−14.5 nT at the beginning of the magnetic cloud.

Figure 1, *a*, *b* indicates that model and observed ΔR behave similarly during the initial and main phases of the storm. During the main phase there is a significant decrease in geomagnetic threshold variations to ΔR_{ef}=−0.69 GV and ΔR_{sgs}=−0.59 GV. Further, during the recovery phase, ΔR_{ef} (Figure 1, *a*) increases, but ΔR_{sgs} (Figure 1, *b*) behaves in a similar way only at low-latitude stations with high threshold rigidities under quiet conditions R_c=6–11 GV (Rome, Almaty, ESOI). At this time, ΔR_{sgs} and ΔR_{ef} differ considerably at the stations with low threshold rigidities R_c=4–1.8 GV (Irkutsk, Moscow, Kingston). The ΔR_{sgs} values at these stations, unlike ΔR_{ef}, continue to decrease for another seven hours after the storm has reached its maximum intensity (minimum Dst on March 9 at 08:00 UT) to minimum ΔR_{sgs}=−1.1 GV at the station Moscow at 15:00 UT. Thus, the maximum decrease in ΔR_{sgs} during the recovery phase is twice as large as the decrease during the storm main phase.

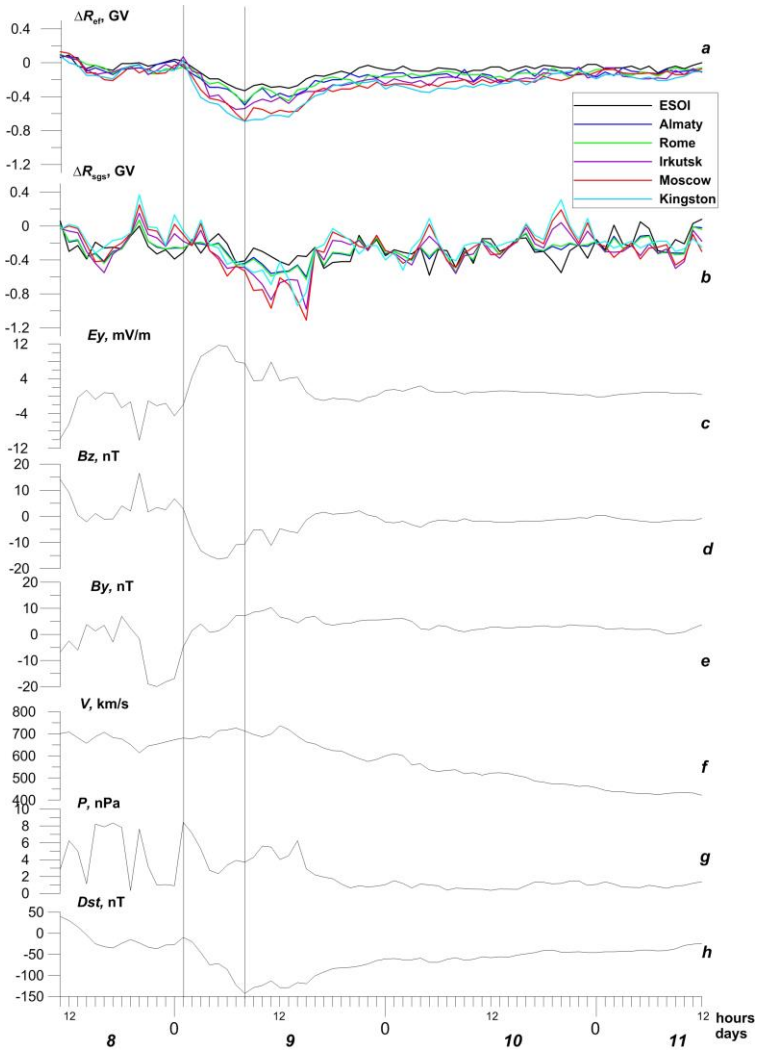

Figure 1. Variations in CR cutoff rigidities ΔR_{ef} (*a*) and ΔR_{sgs} (*b*) at different stations, as well as in IMF parameters E_y (*c*), B_z (*d*), B_y (*e*), SW velocity V (*f*) and pressure P (*g*), and geomagnetic activity index Dst (*h*) during the March 8–11, 2012 geomagnetic storm. Vertical lines indicate the storm main phase

2.2. Latitude dependences

Figure 2 plots ΔR_{sgs} (*a*) and ΔR_{ef} (*b*) as function of R_c at the selected stations located at different latitudes. Latitude curves are given for several moments of storm development: the storm initial phase at *Dst*=−15 nT (I: March 08, 2012, 19:00 UT); the main phase at the storm maximum with *Dst*=−143 nT (II: March 09, 2012, 08:00 UT); the recovery phase with *Dst*=−120 nT (III: March 09, 2012, 15:00 UT), and the next day with *Dst*=−58 nT (IV: March 10, 2012, 12:00 UT).

Figure 2 shows that during the storm initial phase when the disturbance level is low the geomagnetic rigidity variations ΔR obtained by both methods are close to zero at all the stations. During the storm main and recovery phases, ΔR_{ef} and ΔR_{sgs} depend greatly on R_c. The typical latitude curve exhibits a maximum decrease in cutoff rigidity at mid-latitude stations (3–4 GV) during the storm main phase [Dorman, 1963; Flueckiger et al., 1987; Belov et al., 2005; Kress et al., 2010; Danilova et al., 2020]. A characteristic feature of this storm is that ΔR_{sgs} (R_c) forms a latitude curve with a maximum decrease, which is more pronounced during the storm recovery phase (III) than during the main one (II). At the same time, the maximum is shifted to the higher-latitude station Moscow for which R_c=2.39 GV. For ΔR_{ef}, an almost monotonous growth of the curve $\Delta R_{ef}(R_c)$ is observed during the main and recovery phases (a decrease in rigidity variations) with increasing threshold rigidity R_c, i.e. with decreasing latitude of the stations.

2.3. Relationship of geomagnetic thresholds with helio- and geomagnitospheric parameters

To figure out how the obtained CR geomagnetic cutoff rigidity variations are related with the geomagnetic activity, SW, and IMF parameters, we have carried out their correlation analysis for all the stations considered. The findings are presented in Table 2. In the top half of Table 2 are the correlation coefficients *k* for variations in model geomagnetic cutoff rigidities; in the bottom half, for the observed ones. In the last row are the correlation coefficients *k* between ΔR_{ef} and ΔR_{sgs}.

Table 2 shows that the correlation coefficient *k* between ΔR_{ef} and ΔR_{sgs} is very low for the low-latitude station ESOI (R_c=10.8 GV), but with decreasing R_c (increasing latitude) it increases up to *k*=0.68± 0.13 for the station Kingston (R_c=1.88 GV). There is a high degree of correlation between ΔR_{ef} and *Dst* variation (0.88÷0.94). A significant correlation is seen with E_y (−0.65÷-0.75) and B_z (0.63÷0.73) for all the stations. A slightly lower value of *k* (−0.45÷-0.58) is characteristic of the relationship between ΔR_{ef} and B_y. The correlation coefficients *k* between ΔR_{ef} and the SW dynamic parameters *V*, *N*, *P* are low. The correlation coefficient ΔR_{ef} with *P* is the lowest, −0.1 on the average.

The correlation coefficients *k* between ΔR_{sgs} and near-Earth space parameters are somewhat lower than for ΔR_{ef}. This fits the results obtained in the papers comparing model and observed cutoff rigidities for other magnetic storms (e.g., [Ptitsyna et al., 2019] and references therein). Higher degrees of correlation of ΔR_{ef} with *Dst* and SW and IMF parameters are not unexpected since the Ts01 model utilizes *Dst*, SW density *N* and velocity *V*, as well as IMF components as input parameters determining the effect of interplanetary conditions on the magnetosphere and hence on cutoff rigidities.

Then, we plotted correlations of ΔR_{ef} and ΔR_{sgs} with the geoeffective parameters that most significantly affect geomagnetic threshold variations at different stations. For this purpose, Figure 3 shows the correlation coefficients of ΔR with parameters such that $|k|\geq 0.4$.

The above diagrams indicate that the correlation patterns for ΔR_{ef} (Figure 1, *a*) and ΔR_{sgs} (Figure 1, *b*) are similar. The most geoeffective parameters controlling geomagnetic thresholds (both ΔR_{ef} and ΔR_{sgs}) at all latitudes are the geomagnetic activity indices *Dst* and K_p, as well as the azimuthal component of electric field E_y and the IMF southward component B_z. Geoeffectiveness of the SW dynamic parameters *N* and *V* is slightly manifested only for individual stations for ΔR_{ef} (Figure 1, *a*) and is completely absent for ΔR_{sgs} (Figure 1, *b*).

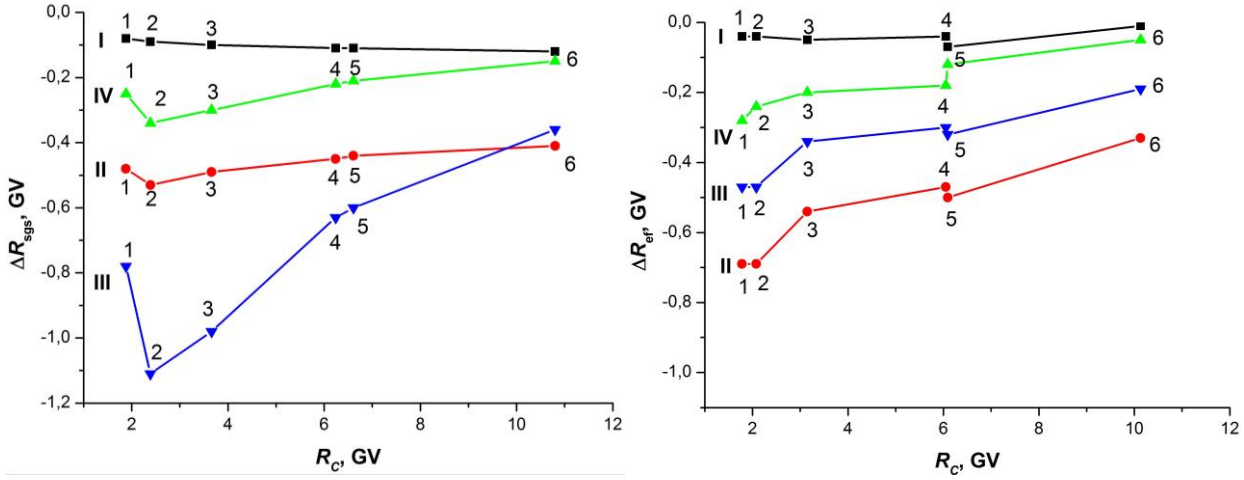

Figure 2. Geomagnetic cutoff rigidity variations ΔR_{sgs} (*a*) and ΔR_{ef} (*b*) as function of threshold rigidity R_c for different magnetospheric activity levels, determined by *Dst*, at time points I–IV of the storm. The stations are designated in order of increasing R_c: 1 — Kingston; 2 — Moscow; 3 — Irkutsk; 4 — Rome; 5 — Almaty; 6 — ESOI

Table 2

Correlation coefficients k between ΔR and geomagnetic activity, SW, IMF parameters

ΔR_{ef}	ESOI	Almaty	Rome	Irkutsk	Moscow	Kingston
Dst	0.88±0.04	0.91±0.05	0.94±0.04	0.92±0.05	0.94±0.06	0.91±0.08
K_p	−0.64±0.07	−0.55±0.09	−0.53±0.09	−0.57±0.12	−0.64±0.13	−0.67±0.13
E_y	−0.73±0.06	−0.72±0.08	−0.65±0.08	−0.71±0.10	−0.71±0.12	−0.75±0.12
B_z	0.71±0.06	0.70±0.08	0.63±0.08	0.69±0.10	0.68±0.12	0.73±0.12
B_y	−0.50±0.08	−0.58±0.09	−0.45±0.10	−0.52±0.12	−0.54±0.14	−0.52±0.15
B	−0.17±0.09	−0.08±0.11	−0.14±0.11	−0.11±0.14	−0.17±0.17	−0.18±0.18
V	−0.40±0.08	−0.31±0.11	−0.33±0.10	−0.32±0.13	−0.42±0.15	−0.41±0.16
N	0.25±0.09	0.35±0.11	0.45±0.10	0.44±0.13	0.38±0.16	0.34±0.17
P	−0.18±0.09	−0.12±0.11	−0.05±0.11	−0.01±0.14	−0.14±0.17	−0.12±0.18
ΔR_{sgs}	ESOI	Almaty	Rome	Irkutsk	Moscow	Kingston
Dst	0.42±0.13	0.64±0.10	0.66±0.10	0.65±0.16	0.65±0.19	0.64±0.17
K_p	−0.31±0.13	−0.46±0.12	−0.47±0.12	−0.46±0.18	−0.46±0.22	−0.41±0.20
E_y	−0.18±0.14	−0.41±0.12	−0.42±0.12	−0.48±0.18	−0.50±0.22	−0.47±0.19
B_z	0.17±0.14	0.40±0.12	0.42±0.12	0.48±0.18	0.49±0.21	0.48±0.19
B_y	−0.11±0.14	−0.32±0.13	−0.33±0.13	−0.41±0.19	−0.43±0.22	−0.43±0.20
B	−0.03±0.14	−0.02±0.13	−0.03±0.14	−0.04±0.20	−0.06±0.25	0±0.22
V	−0.25±0.14	−0.33±0.13	−0.34±0.13	−0.30±0.20	−0.28±0.24	−0.26±0.21
N	0.21±0.14	0.25±0.13	0.24±0.13	0.19±0.20	0.18±0.24	0.21±0.21
P	0±0.14	−0.13±0.13	−0.14±0.14	−0.20±0.20	−0.18±0.24	−0.12±0.22
K	0.35±0.08	0.60±0.09	0.60±0.09	0.64±0.11	0.66±0.13	0.68±0.13

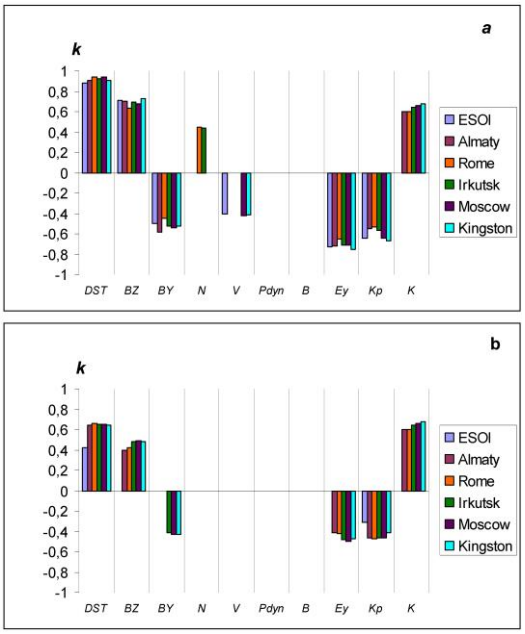

Figure 3. Diagrams of correlation of CR geomagnetic threshold variations with IMF, SW, and geomagnetic activity parameters for which $|k|\geq 0.4$: *a* — ΔR_{ef}; *b* — ΔR_{sgs}

3. DISCUSSION

Our results show that during the strong magnetic storm on March 8–11, 2012 the highest degree of correlation of ΔR was with *Dst*, as well as with B_z and E_y. The fact that the geomagnetic threshold variation (both ΔR_{sgs} and ΔR_{ef}) correlates most closely with *Dst* suggests that the ring current plays the main role in controlling CR geomagnetic cutoff rigidity variations during all storm phases. Significant sensitivity to *Dst*, which has been observed in [Ptitsyna et al., 2019], is the most stable feature of the interaction between geomagnetic threshold variations and the geomagnetosphere. In the same work, it has been shown that the relationship of ΔR with geomagnetic activity demonstrates a clear regularity — the correlation increases with decreasing *Dst*, i.e. with increasing storm intensity.

It is believed that the reconnection between the SW magnetic field and the geomagnetospheric field, as well as the SW dynamic pressure *P*, responsible for magnetosphere compression, play the main role in the development of magnetospheric disturbances [Dungey, 1961; Akasofu, 1981; Russell, 2000]. Both of these factors weaken the geomagnetic shielding, reduce the geomag-

netic cutoff rigidity, and facilitate SW plasma penetration into Earth's magnetosphere and atmosphere. For the March 2012 storm, we have found that the SW pressure P has almost no control over geomagnetic cutoff rigidity variations. The southward turn of the B_z component and the resulting magnetic reconnection generated the geomagnetic storm. The further decrease in B_z led to a weakening of geomagnetic shielding and a decrease in ΔR_{sgs} and ΔR_{ef} during the main phase of the storm. The high degree of influence of E_y we have obtained on geomagnetic cutoff rigidity variations ΔR_{sgs} and ΔR_{ef}, derived by both methods, supports the viewpoint that the azimuthal electric field is one of the most geoeffective SW parameters (see, e.g., [Burton et al., 1975] and references therein). Borovsky and Birn [2014] believe that SW electric field penetration along magnetic field lines after SW field lines get connected to Earth's polar cap due to reconnection may become an important factor in controlling geomagnetic current systems during later phases of storm development.

Thus, the results obtained by the two fundamentally different methods show good agreement, which increases confidence in them.

The difference found between variations in ΔR_{sgs} and ΔR_{ef} during later storm phases (see Figure 1, *a*, *b*) requires separate consideration. To compare CR cutoff rigidities, obtained by various methods, most objectively, it is necessary to involve direct satellite measurements, yet there are very few such works. In one of such studies [Adriani et al., 2016], CR cutoff rigidity variations were directly measured by the PAMELA spacecraft during a 2006 storm. Variations in the cutoff latitude as function of ΔR were studied at relatively short time intervals corresponding to the orbital period of the spacecraft (~94 min). Comparison of the satellite experiment results with the rigidities obtained by the Ts96 model and the more advanced Ts05 model has shown that the cutoff rigidities (cutoff latitude) from satellite data differ from ΔR_{ef}. The cutoff latitude obtained by the models is systematically shifted to the equator as compared to experimental satellite data (by ~21 % for the Ts96 model and by ~18 % for the Ts05 model).

For the March 2012 storm under study, ΔR_{ef} decreases during the main phase, reaches a minimum (−0.69 GV) at storm maximum (March 9 at 08:00 UT), and then increases during the storm recovery phase. As for ΔR_{sgs}, similar behavior is observed only at low-latitude stations (ESOI, Almaty, Rome). At high-latitude stations, ΔR_{sgs} behaves differently, it continues to decrease for seven hours after the storm maximum, and reaches a minimum (−1.1 GV) at the station Moscow on March 9 at 15:00 UT, during the storm recovery phase. Thus, the decrease in ΔR_{sgs}, i.e. suppression of geomagnetic shielding at subauroral latitudes (Moscow and Irkutsk), was twice as strong during the storm recovery phase as during the main phase. This atypical behavior of ΔR_{sgs} is likely related to the intense substorm activity recorded during the recovery phase of the geomagnetic storm. According to [Despirak et al., 2021], on March 9 at 9:00–16:00 UT there was a sharp increase in the westward electrojet in the form of several consecutive very intense large-scale substorms (supersubstorms) with an amplitude of ~2500 nT. Despirak et al. [2021] attribute the development of such supersubstorms to precipitation of intense charged particle fluxes from the magnetotail. During very intense substorms, currents over 1–2 mA occur which significantly change the configuration of the magnetic field of the magnetosphere [Nikolaev et al., 2015]. The weakening of geomagnetic shielding during the recovery phase (8:00–15:00 UT) might have been caused by the formation of the current system of supersubstorms.

The Ts01 model, developed from satellite observations in the magnetosphere, is known to be able to describe the averaged configuration of the magnetospheric field, yet it does not describe relatively fast dynamic processes such as substorms [Pchelkin, 2010; Nikolaev et al., 2015]. Thus, suppression of geomagnetic shielding during the storm recovery phase at sharp intensification of westward electrojet currents is not reflected in ΔR_{ef}, whereas ΔR_{sgs} can respond to various changes in the magnetic field of the magnetosphere at all latitudes. Despirak et al. [2021] note the complexity of the observed pattern when during the recovery phase of one supersubstorm the phase of the next one develops, which makes it difficult to distinguish individual substorms of very large amplitude. Two strong jumps in ΔR_{sgs} at high latitudes on March 9 at ~12:00 and 15:00 UT seem to reflect these complex changes in the configuration of the magnetospheric magnetic field, which are caused by the formation of several successive supersubstorms.

It might be the differences in sensitivity of the two methods to supersubstorms that explain the difference in the behavior of ΔR_{sgs} and ΔR_{ef} during the recovery phase of the storm under study. This assumption, however, requires additional verification.

CONCLUSION

During the active interval of CAWSES-II, four consecutive geomagnetic storms were observed. We have analyzed a decrease in CR geomagnetic cutoff rigidity variations occurring during the strongest storm on March 8–11, 2012 and their dependence on SW, IMF, and geomagnetic activity parameters. The obtained predominant correlation between ΔR and *Dst* suggests that the geomagnetic threshold variations during the storm under study are generally driven by the ring current. Furthermore, we have obtained a high degree of correlation of ΔR with the electromagnetic parameters B_z and E_y. The dynamic SW parameters have almost no effect on cutoff rigidity variations. These conclusions have been drawn using fundamentally different methods of calculating ΔR, which increases confidence in them. A feature of the storm is that ΔR_{sgs} at high-latitude stations reach a minimum not at storm maximum, as ΔR_{ef} does, but seven hours later, already during the recovery phase. This fact may be associated with the development of several supersubstorms at that time, which had a high amplitude and global spatial scales. We assume that the difference in the behavior of the model and observed ΔR values during the storm recovery phase might have arisen due to the fact that the Ts01 model describes the aver-

aged configuration of the magnetospheric field, not an individual supersubstorm. This assumption, however, requires additional research.

We are grateful to the anonymous reviewer for the comments.

The work was financially supported by the Ministry of Science and Higher Education of the Russian Federation. The results were obtained using the equipment of Shared Equipment Center "Angara" [http://ckp-rf.ru/ckp/3056] and the Unique Research Facility "Russian National Ground-Based Network of Cosmic Ray Stations" (CRS Network) [https://ckp-rf.ru/usu/433536].

REFERENCES

Adriani O., Barbarino G.C., Bazilevskaya G.N., Bellotti R., et al. PAMELA's measurements of geomagnetic cutoff variations during the 14 December 2006. *Space Weather*. 2016, vol. 14, no. 3. DOI: 10.1002/2016SW001364.

Akasofu S.I. Energy coupling between the solar wind and the magnetosphere. *Space Sci. Rev*. 1981, vol. 28, pp. 121–190. DOI: 10.1007/BF00218810.

Belov A., Baisultanova L., Eroshenko E., Mavromichalaki H., Yanke V., Pchelkin V., Plainaki, C., Mariatos G. Magnetospheric effects in cosmic rays during the unique magnetic storm on November 2003. *J. Geophys. Res*. 2005, vol. 110, A09S20. DOI: 10.1029/2005JA011067.

Borovsky J.E., Birn J. The solar wind electric field does not control the dayside reconnection rate. *J. Geophys. Res.: Space Phys*. 2014, vol. 119. DOI: 10.1002/2013JA019193.

Burton R.K., McPherron R.L., Russel C.J. An empirical relationship between interplanetary conditions and *Dst. J. Geophys. Res*. 1975, vol. 80, pp. 4204–4214.

Carslaw K.S., Harrison R.G., Kirkby J. Cosmic rays, clouds, and climate. *Science*. 2002, vol. 298, iss. 5599, pp. 1732–1737. DOI: 10.1126/science.1076964.

Danilova O.A., Ptitsyna N.G., Tyasto M.I., Sdobnov V.E. Disturbed magnetosphere on November 7–8, 2004 and variations of cosmic ray cutoff rigidity: Latitude effects. *Solar-Terr. Phys*. 2020, vol. 6, iss. 3, pp. 43–50. DOI: 10.12737/stp-63202005.

Despirak I.V., Lyubchich A.A., Kleimenova N.G., Gromova L.I., Gromov S.V., Malysheva L.M. Longitude geomagnetic effects of the supersubstorms during the magnetic storm of March 9, 2012. *Bull. Russ. Acad. Sci. Phys.* 2021, vol. 85, pp. 246–251. DOI: 10.3103/S1062873821030096.

Dorman L.I. *Elementary Particle and Cosmic Ray Physics*. New York, Elsevier Publ., 1963, 456 p.

Dungey J.W. Interplanetary magnetic field and the auroral zones. *Phys. Rev. Lett*. 1961, vol. 6, pp. 47–48. DOI: 10.1103/PhysRevLett.6.47.

Dvornikov V.M., Kravtsova M.V., Sdobnov V.E. Diagnostics of the electromagnetic characteristics of the interplanetary medium based on cosmic ray effects. *Geomagnetism and Aeronomy*. 2013, vol. 53, iss. 4, pp. 430–440.

Kress B.T., Mertens C.J., Wiltberger M. Solar energetic particle cutoff variations during the 29–31 October 2003 geomagnetic storm. *Space Weather*. 2010, vol. 8, S05001. DOI: 10.1029/2009SW000488.

Flueckiger E.O., Shea M.A., Smart D.F. On the latitude dependence of cosmic ray cutoff rigidity variations during the initial phase of a geomagnetic storm. *Proc. 20th Int. Conf. Cosmic Rays*. Moscow, 1987, vol. 4, pp. 2016–2020.

Makrantoni P., Mavromichalaki H., Usoskin I., Papaioannou A. Calculation of the cosmic ray induced ionization for the region of Athens. *Journal of Physics: Conference Series*. 2013, vol. 409, iss. 1, 012232. DOI: 10.1088/1742-6596/409/1/012232.

Nikolaev A.V., Sergeev V.A., Tsyganenko N.A., Kubyshkina M.V., Opgenoorth H., Singer H., Angelopoulos V. A quantitative study of magnetospheric magnetic field line deformation by a two-loop substorm current wedge. *Ann. Geophys*. 2015, vol. 33, pp. 505–517. DOI: 10.5194/angeo-33-505-2015.

Pchelkin V.V. Effect of magnetospheric substorms on asymptotic directions of arrival of cosmic ray relativistic protons. *Geomagnetism and Aeronomy*. 2010, vol. 50, pp. 314–319. DOI: 10.1134/S0016793210030059.

Ptitsyna N.G., Danilova O.A., Tyasto M.I., Sdobnov V.E. Influence of the solar wind and geomagnetic activity parameters on variations in the cosmic ray cutoff rigidity during strong magnetic storms. *Geomagnetism and Aeronomy*. 2019, vol. 59, no. 5, pp. 530–538. DOI: 10.1134/S0016793219050098.

Ptitsyna N.G., Danilova O.A., Tyasto M. I. Correlation of the cosmic-ray cutoff rigidity with heliospheric and geomagnetic-activity parameters at different phases of a magnetic storm in November 2004. *Geomagnetism and Aeronomy*. 2020, vol. 60, no. 3, pp. 268–278. DOI: 10.1134/S0016793220020139.

Ptitsyna N.G., Danilova O.A., Tyasto M.I., Sdobnov V.E. Dynamics of cosmic-ray cutoff rigidity and magnetospheric parameters during different phases of the storm of November 20, 2003. *Geomagnetism and Aeronomy*. 2021, vol. 61, no. 2, pp. 169–179. DOI: 10.1134/S0016793221010114.

Russell C.T. The solar wind interaction with the Earth's magnetosphere: A tutorial. *IEEE Trans. Plasma Sci*. 2000, vol. 28, no. 6, pp. 1818–1830. DOI: 10.1109/27.902211.

Shea M.A., Smart D.F., McCracken K.G. A study of vertical cutoff rigidities using sixth degree simulations of the geomagnetic field. *J. Geophys. Res*. 1965, vol. 70, pp. 4117–4130.

Tsurutani B., Echer E., Shibata K., Verkhoglyadova O., Mannucci A., Gonzalez W., Kozyra J., Pätzold M. The interplanetary causes of geomagnetic activity during the 7–17 March 2012 interval: a CAWSES II overview. *J. Space Weather Space Clim*. 2014, vol. 4, A02. DOI: 10.1051/swsc/2013056.

Tsyganenko N.A., Singer H.J., Kasper J.C. Storm-time distortion of the inner magnetosphere: How severe can it get? *J. Geophys. Res*. 2003, vol. 108, iss. A5, 1209. DOI: 10.1029/2002JA009808.

URL: http://www01.nmdb.eu/data (accessed February 20, 2023).

URL: https://omniweb.gsfc.nasa.gov/form/dx1.html (accessed July 3, 2015).

URL: http://ckp-rf.ru/ckp/3056 (accessed February 20, 2023).

URL: https://ckp-rf.ru/usu/433536 (accessed February 20, 2023).

This paper is based on material presented at the 18th Annual Conference on Plasma Physics in the Solar System, February 6–10, 2023, IKI RAS, Moscow.

Original Russian version: Danilova O.A., Ptitsyna N.G., Tyasto M.I., Sdobnov V.E., published in Solnechno-zemnaya fizika. 2023. Vol. 9. Iss. 2. P. 86–93. DOI: 10.12737/szf-92202310. © 2023 INFRA-M Academic Publishing House (Nauchno-Izdatelskii Tsentr INFRA-M)

How to cite this article

Danilova O.A., Ptitsyna N.G., Tyasto M.I., Sdobnov V.E. Variations in cosmic ray cutoff rigidities during the March 8–11, 2012 magnetic storm (CAWSES II period). *Solar-Terrestrial Physics*. 2023. Vol. 9. Iss. 2. P. 81–87. DOI: 10.12737/stp-92202310.